PHOTONIC SENSORS / Vol. 10, No. 2, 2020: 134–146

A Numerical Approach to Design the Kretschmann Configuration Based Refractive Index Graphene-MoS_2 Hybrid Layers With TiO_2-SiO_2 Nano for Formalin Detection

Md. Biplob HOSSAIN[1*], Tamanna TASNIM[2], Lway F. ABDULRAZAK[3], Md. Masud RANA[2], and Md. Rabiul ISLAM[4]

[1]*Department of Electrical and Electronic Engineering, Jashore University of Science and Technology, Jashore-7408, Bangladesh*

[2]*Department of Electrical and Electronic Engineering, Rajshahi University of Engineering & Technology, Rajshahi-6402, Bangladesh*

[3]*Department of Computer Science, Cihan University Slemani, Sulaimaniya-46001, Iraq*

[4]*School of Electrical Computer and Telecommunications Engineering, Faculty of Engineering and Information Sciences, University of Wollongong, NSW 2522, Australia*

[*]Corresponding author: Md. Biplob HOSSAIN E-mail: biplobh.eee10@gmail.com

Abstract: In this paper, a Kretschmann configuration based surface plasmon resonance (SPR) sensor is numerically designed using graphene-MoS_2 hybrid structure TiO_2-SiO_2 nano particles for formalin detection. In this design, the observations of SPR angle versus minimum reflectance and SPR frequency (F_{SPR}) versus maximum transmittance (T_{max}) are considered. The chitosan is used as probe legend to perform reaction with the formalin (40% formaldehyde) which acts as target legend. In this paper, both graphene and MoS_2 are used as biomolecular acknowledgment element (BAE) and TiO_2 as well as SiO_2 bilayers is used to improve the sensitivity of the sensor. The numerical results show that the variation of FSPR and SPR angles for inappropriate sensing of formalin is quite insignificant which confirms the absence of formalin. On the other hand, these variations for appropriate sensing are considerably significant that confirm the presence of formalin. At the end of this article, the variation of sensitivity of the proposed biosensor is measured in corresponding to the increment of a refractive index with a refractive index step 0.01 refractive index unit (RIU). In inclusion of TiO_2-SiO_2 bilayers with graphene-MoS_2, a maximum sensitivity of 85.375% is numerically calculated.

Keywords: Surface plasmon resonance formalin detection; grapheme; refractive index; sensitivity

Citation: Md. Biplob HOSSAIN, Tamanna TASNIM, Lway F. ABDULRAZAK, Md. Masud RANA, and Md. Rabiul ISLAM, "A Numerical Approach to Design the Kretschmann Configuration Based Refractive Index Graphene-MoS_2 Hybrid Layers With TiO_2-SiO_2 Nano for Formalin Detection," *Photonic Sensors*, 2020, 10(2): 134–146.

1. Introduction

Formalin is an ecologically extensively chemical compound that causes cancer to humans [1]. Exposure to formalin will possibly cause antagonistic health effects. It is the greatest practical contact allergen in metal working fluids [1]; toxic incident can cause ecological hypersensitivity and

Received: 7 March 2019 / Revised: 16 June 2019

DOI: 10.1007/s13320-019-0566-5
Article type: Regular

chronic worsening disease [1]. Formalin is a poisonous element which contains 40% formaldehyde soluble in water [2]. Formaldehyde travels the blood throughout the body and rejoins with proteins, abolishing their biological function. Also, it can react with an amine functional group of the amino acid lysine in a protein, called rhodopsin. Formaldehyde also reacts with amino groups in other proteins, including many enzymes, and the loss of the function of these biological catalysts causes death [1]. Recent news and research have explored the frequent use of formaldehyde in food preservation, which is very popular, particularly in Asian region [2]. Therefore, the accurate detection of formalin is a serious national issue, which is a biochemical process. Its mechanism of action for fitting deceits in its aptitude to form cross-links between soluble and structural proteins. The resulting structure holds its cellular constituents in them in vivo associations to each other, giving it a degree of mechanical strength, which permits it to survive subsequent processing [3].

Many conventional procedures are available for the detection of formaldehyde, enzyme detection, food safety, and environmental monitoring [4–7]. These procedures are Deniges and Eegriwes methods [4], gas chromatography-mass spectrometry (GC-MS) [5], high performance liquid chromatography (HPLC) [6], fluorimetry [7], Nash test [7], gravimetric methods [6], and other chemical based procedures. Unfortunately, these methods, reagents, and reaction products are often harmful to human health. The conventional methods require similarly hazardous reagents and suffer from a number of interferences, resulting in false positions. Additionally, conventional methods are impracticable for real-time measurements [1]. To overcome the drawbacks of the conventional procedures and meet the requirement of concerned issue, the biosensor technology can play a significant role in the solution.

In recent years, refractive index based surface plasmon resonance (SPR) bio-sensing has been widely researched because this sensor technology has a great potential for detection and analysis of chemical and biochemical substances in many important areas including medicine, biotechnology, monitoring of drug, food quality, environment safety, formalin detection, medical diagnosis, enzyme detection, and doxyribonucleic acid (DNA-DNA) hybridization [8–19].

The collective oscillation of metallic electrons in the presence of time varying electromagnetic field at the meta-dielectric interface is defined as SPR [19–25]. Plasmons are stand-alone solutions of Maxwell's equations consisting in collective excitations of charge, which move coherently with a common frequency and wave-vector [19]. While bulk plasmons are related to bulk systems, surface plasmons waves (SPW) that propagate along the metal-dielectric interface [19–22]. When the phase matching condition between incident wave and surface plasmons wave is satisfied, the externally shined light gets coupled with the surface plasmon modes of the metal-dielectric interface giving birth to the propagating oscillation in the longitudinal direction and evanescently decaying in transverse directions [19]. The condition of phase matching is found to be met only with the transverse magnetic (TM) polarization mode of the incident light [26]. Since the direct light does not carry enough momentum to excite surface plasmons at the desired interface, Kretschmann configurations have been proposed to provide light the extra momentum [22–25]. In these configurations, the light gets its extra momentum from the high refractive index of the dielectric material of prism [20]. The SPR technique is successfully applied to detect the presence of formalin in sample biomolecules.

Numeral SPR biosensors have been industrially advanced, and among them the compact surface plasmon (CSPR) sensor [27], the optical sensing surface plasmon resonance (OSSPR) sensor [28], the localized surface plasmon resonance (LSPR) sensor

[29, 30], and the long-range surface plasmon resonance (LRSPR) sensor [31, 32] have the benefits of compactness, lightness in weight, high sensitivity, the case of multiplexing and remote sensing, and so on. Fundamentally, there is no major difference in operating principle among the above-mentioned sensors. LRSPRs are surface electromagnetic waves that can be created on thin metallic films entrenched between two identical refractive index dielectrics [31, 32], on the other hand, LSPR can be used on the metal-dielectric interface with different refractive indexes to generate SPW [29, 30]. In LSPR, the variation of the concentration of biomolecules owing to chemical reaction will make a local change of surrounding refractive index near the sensor surface [29]. This change of refractive index results in a change of propagation constant of the SPW and thus the SPR angle and SPR frequency (F_{SPR}) change [10]. The principle of OSSPRs is the same with LSPRs except that it is fabricated in optical fiber cables [12, 17, 28]. Compared with these SPR biosensors, the LRSPRs have longer surface propagation lengths, higher surface electric field strengths, and narrower angular resonance curves [32]. The LSPRs offer better sensitivity, robustness, and facile detection [29]. OSSPRs accept the benefits of remote sensing applications [33].

One of the key ingredients of any sensing device is the binding/adsorbing material with a large surface area [9, 14, 21], and the graphene and MoS_2 have attracted a considerable amount of attention interestingly because of their large band gap [14], high optical absorption efficiency [34, 35], and large work function [12]. Titanium dioxide (TiO_2) is one of the most widely used semiconductors in photo catalysis and solar energy conversion [22]. As an SPR sensitive material, it has distinguished advantages such as low cost, high stability, high permittivity, and environmental friendliness [16, 18, 36, 37]. The silicon dioxide (SiO_2) layer also increases the sensitivity of the probe [16, 18, 38, 39]. The porous TiO_2 & SiO_2 film gives us a huge surface area to maximize the amount of incident light that can be absorbed. For this reason, TiO_2-SiO_2 nano particles show tremendous plasmonic effect near TiO_2-SiO_2 interface facilitating effective light trapping. This effective light trapping generates more surface plasmons (SPs) which will eventually enhance the SPR angle and frequency. This rise of SPR angle and frequency will increase the sensor sensitivity [16, 38].

In the current study, numerical Kretschmann configuration based refractive index sensor utilizing graphene-MoS_2 hybrid layers with TiO_2-SiO_2 nano particles is designed and investigated, which can explore a new window for the detection of formalin. A composite graphene-MoS_2-Au-TiO_2-SiO_2 layer is used for faster immobilization by monitoring the change of SPR angle-minimum reflectance attributor and SPR frequency-maximum transmittance attributor. Finally, the influence of adding TiO_2-SiO_2 with graphene-M_OS_2 is investigated, which results in a higher sensor sensitivity of 85.375% compared with the conventional structure reported. At the end of this article, a study of the variation of sensitivity of the proposed biosensor is measured in corresponding to the increment of a refractive index with a refractive index step 0.01 refractive index unit (RIU).

2. Methodology and theoretical design strategy

The proposed SPR biosensor is composed of seven layers, of which the configuration is shown in Fig. 1. The incident light in the transverse magnetic (TM) polarization state is the most important condition for excitation of SPs [22]. For an inciting TM polarized light, a polarizer is used in the way of incident. For the angular interrogation method, the Kretschmann arrangement based sensor, this paper considers the Fresnel optical system to design the proposed sensor which was discussed in detail in [9–16]. To give extra momentum to the incident

light, high wave vector photonic crystals need to be used [40]. So to fulfil this condition, we specify high refractive indexed prism, such as SF11 glass prism, as a base layer having a high refractive index (n_p), which is shown in Table 1. In this paper, gold is used to maintain good resistance from oxidation and corrosion, better chemical stability, and superior optical performances [9, 22]. A resonant excitation of photon-electron coupling takes place when the wave vector of the incident light remains confined at the interface and decays exponentially in the transverse directions [14, 41].

Table 1 Sensor layers' description with the optimized material's geometries.

Position	Layer materials	Refractive index (n) (RIU)	Optimized thickness (d) (nm)	References
1st	SF11 glass prism	n_1=1.7786	---	[12, 18]
2nd	Porous TiO_2	n_2=2.5837	d_2=37	[16, 18]
3rd	Porous SiO_2	n_3=1.4570	d_3=20	[16, 18]
4th	Gold (Au)	n_4=0.1838 +i3.4313	d_4=20	[9, 11, 14, 22]
5th	MoS_2	n_5=5.9+i0.8	d_5=0.65	[18, 39]
6th	Graphene	n_6=3.0 + i1.1487	d_6=0.34	[42–44]
7th	PBS solution	n_7=1.34	----	[45, 46]

The evanescent tail of SPR is very sensitive to changes in a complex refractive index of a metal layer, surrounding dielectric medium, and their geometrical sizes [14, 22], which results in high sensor sensitivity [22]. For accelerating sensitive changes of tail in SPR evanescent wave to obtain a high sensor sensitivity, we select graphene and MoS_2 which have high complex refractive index as well as high carrier mobility, high optical transparency, exceptional mechanical flexibility, mechanical strength, low resistivity, tunable conductivity, and extreme mode confinement [47–50]. And the final layer is phosphate buffer saline (PBS) solution as bare sensing dielectric medium, which affords better adsorption of biomolecules [45, 46]. A complete theoretical configuration of the proposed sensor with the optimized material's geometries has been summarized in Table 1. After confirming the setup, a TM polarized He-Ne light with a wavelength of 633 nm is used, which passes through the prism and some portion is reflected at the composite layer interface.

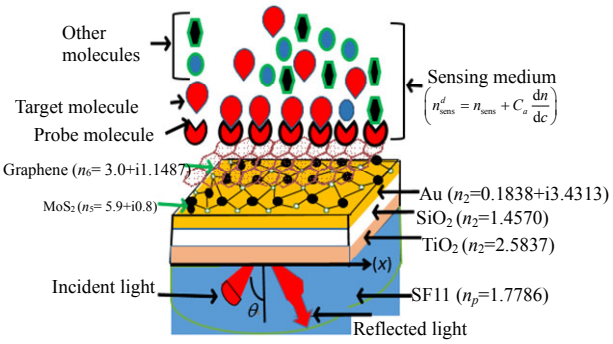

Fig. 1 Schematic diagram of the proposed SPR biosensor, where the MoS_2 layer is coated on Au film (thickness d_{Au} is 50 nm to maintain both high detection accuracy and quality factor we have considered gold layer thickness of 50 nm throughout the analysis. Another point would be the fluctuating nature of SPR angle except 50 nm, which suggests difficulty to find out a stable sensing stage) and monolayer graphene is coated on the lower MoS_2 layer as the biomolecular recognition element.

At the time of ongoing light energy to composite layer interface, an evanescent momentary wave is produced which is known as SPW mentioned in the section that propagates with a dissimilar propagation constant from light wave. The propagation constant of SPW can be adjusted in such a way that it equals to the propagation constant of optical wave in order to obtain surface resonance. The point at which the optical wave propagation constant equals to the SPW propagation constant is called SPR point [12]. As expressed in (1), the SPR angle is a refractive index dependent parameter of the sensing medium. At the SPR point, the frequency at which SPW propagates is called surface plasmon resonance frequency (F_{SPR}) [10] and the angle of incidence is called SPR angle [10–12] that can be expressed by (1) [12, 16, 18]:

$$\theta_{SPR} = \sin^{-1} \frac{(n_{eff} n_{sens})}{n_{prism} \sqrt{\left(n^2_{eff} + n^2_{sens}\right)}} \quad (1)$$

where n_{prism} and n_{sens} are the refractive indexes of SF11 glass prism (n_1=1.7786) and sensing dielectric medium (n_7=1.34 for PBS in bare sensor), respectively; n_{eff} refers to the equivalent refractive index of Graphene-MoS_2-Au metallic with

TiO_2-SiO_2 nano composite layers which are defined in [12, 16, 18]. When formalin is fleeting into chitosan on the sensor medium, the refractive index of sensing medium is modified owing to performing chemical reaction between chitosan and formalin as follows [10, 12, 15]:

$$\Delta n_{\text{sens}} = n_{\text{sens}}^{d} - n_{\text{sens}} = \left(n_{\text{sens}} + C_a \frac{\mathrm{d}n}{\mathrm{d}c} \right) - n_{\text{sens}} = C_a \frac{\mathrm{d}n}{\mathrm{d}c} \tag{2}$$

where n_{sens}^{d} is the refractive index of the sensing dielectric medium after adsorption of formaldehyde molecules, n_{sens} is the refractive index of the sensing dielectric medium before adsorption of formaldehyde molecules and is equal to the refractive index of PBS saline, C_a is the concentration of adsorbed biomolecules for example 1000 nM formaldehyde solution, and dn/dc is the refractive index increment factor. For PBS, the increment factor is 0.181 cm^3/gm [12, 16, 18, 51]. If a change in the SPR angle is found, a change in the propagation constant of SPW has been found which is explained mathematically in [10] as given below:

$$K_{\text{SPW}} = \frac{2\Pi}{\lambda} n_{\text{prism}} \sin\theta_{\text{SPR}} . \tag{3}$$

Finally, F_{SPR} is changed due to the change in the propagation constant of SPW which can be explained by the following equation [10, 16, 18]:

$$F_{\text{SPR}} = \frac{K_{\text{SPW}}}{2\Pi} \frac{C_o}{n_{\text{eff}}} \tag{4}$$

where C_o / n_{eff} is the propagation velocity of SPW that is a perpendicularly confined evanescent electromagnetic wave [52–54]. If the SPR angle of optical wave is tuned, SPR condition is achieved, where reflectance (R) of reflected wave is the minimum and transmittance (T) is the maximum and then SPW penetrates at F_{SPR} along the x-direction. We define two plots "transmittance versus surface resonance frequency (T~F_{SPR} curve)" as well as "reflectance versus surface resonance angle (R~θ_{SPR} curve)" as surface resonance detecting attributors. To make these curves, we use Fresnel equation for the seven-layer hetero optical system to determine reflected and transmitted light intensities discussed elaborately in [9–12, 14, 21, 22].

3. Numerical results analysis

3.1 Formalin detection approach

In this paper, Formaldehyde is detected by interacting with Chitosan and biomolecular components. Therefore, when a chemical bond is formed with the probe which is attached to the target component, it forms additional bonding which shows peculiar phenomena. From the response of the phenomena, one can easily determine that the sample contains formalin or not. This section is based on the tabulated value of concentration for the minimum reflectance & SPR angle along with the SPR frequency and maximum transmittance which helps detect formalin successfully. Here, we discuss in detail how dose our proposed biosensor distinguish from the presence of formaldehyde in the sensing solution. Firstly, a numerical analysis is initiated by checking the R~θ_{SPR} and T~F_{SPR} curves in the absence of both formalin (target ligand) and chitosan (probe ligand), which is normally known as bare sensor, as shown in Fig. 2. In our proposed SPR device, PBS is used as a sensing medium that helps measure the dependency of reflectance on θ_{SPR} and transmittance on F_{SPR}. The work is continued by assuming that our sensor is susceptible of differentiating between probe element (chitosan) and detectable target (formalin) with regard to the analysis of detection. It is noticeable that an increase in the SPR angle and SPR frequency towards the right side of R~θ_{SPR} and T~F_{SPR} curve is found due to the use of nano film TiO_2-SiO_2 layers, whose phenomenon accounts for enhanced sensitivity [39].

Figures 2(a) and 2(b) illustrate the R~SPR angle and T~F_{SPR} curve. The blue line in Figs. 2(a) and 2(b) shows the SPR angle (56.26°) and F_{SPR} (97.968 THz) during both probe (chitosan) and target (formalin), which are absent respectively in the sensor. The SPR

angle and F_{SPR} of bare sensor are 56.26° and 97.968 THz, respectively. The red line in Fig. 2(a) shows the SPR angle (56.34°) and the green line in Fig. 2(b) shows F_{SPR} (98.688 THz), while 1000 nM probe (chitosan) is presented in PBS.

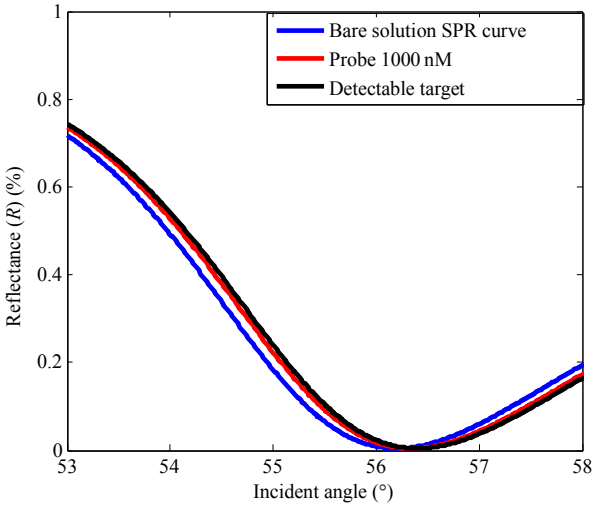

(a)

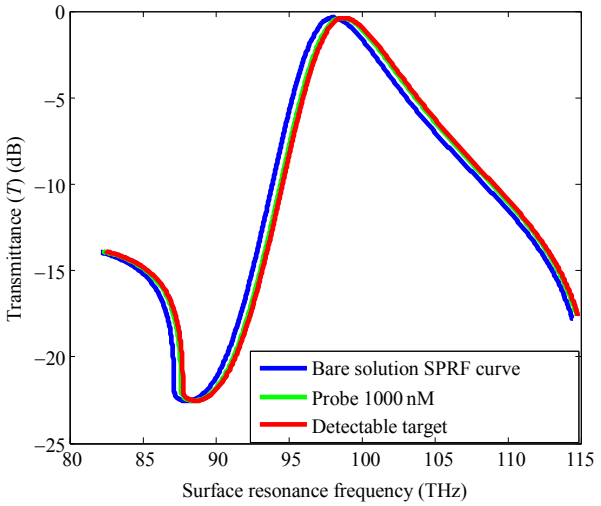

(b)

Fig. 2 SPR imaging curve of bare sensor: (a) R~θ_{SPR} curves and (b) T~F_{SPR} curves in the absence of formalin and presence of chitosan.

Secondly, we observe the change of detecting attributors ($\Delta\theta_{SPR}$ & R_{min}) and (ΔF_{SPR} & T_{max}) due to adding different concentrated formalin as shown in Fig. 3, and these changed are provided in Table 2. The data of Table 2 are extracted from Figs. 3(a) and 3(b), respectively.

Table 2 Data of detecting attributors R_{min} (%), θ_{SPR} (deg), T_{max} (dB) and F_{SPR} (THz) for different concentrated formalin ranging from 1000 nM to 1200 nM.

Concentration	R_{min} (%)	θ_{SPR} (°)	T_{max} (dB)	F_{SPR} (THz)
1000 (Immobilizer probe)	0.0044	56.3400	0.3795	98.688
1000 (Detectable target)	0.0062	58.0500	0.3981	99.875
1001 (Detectable target)	0.0066	58.3800	0.4002	100.008
1010 (Detectable target)	0.0070	58.6700	0.4018	100.106
1100 (Detectable target)	0.0082	59.4900	0.4106	100.627
1110 (Detectable target)	0.0085	59.6800	0.4129	100.761
1200 (Detectable target)	0.0100	60.6200	0.4249	101.447

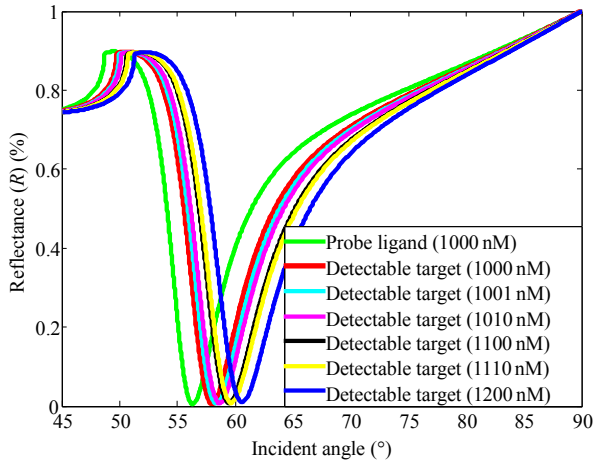

(a)

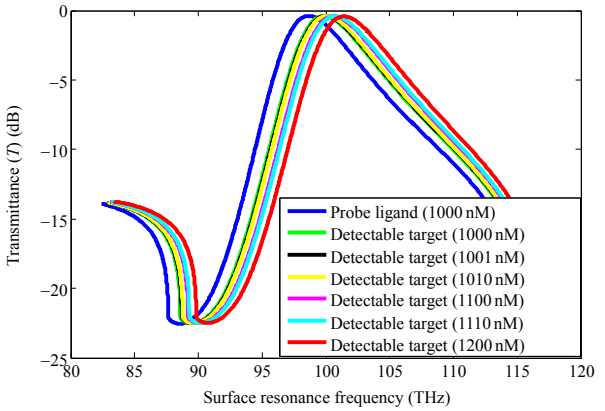

(b)

Fig. 3 SPR imaging curve of proposed sensor: (a) R~θ_{SPR} curves and (b) T~F_{SPR} curves for different concentrated detectable targets.

Since the change of concentration is due to the immobilization of chitosan within the sensing medium, the local refractive index of the sensing medium is also changed followed by (2). Equation (1) states that the SPR angle changes if n_{sens} changes, which finally translates a change in K_{SPW} observed from (3). At the transition point where the SPW

wave vector and optic wave vector are equal, the minimum reflectance ($R_{\min}$) and maximum transmittance ($T_{\max}$) are found. As illustrated in Fig. 2, before reaction of formalin with chitosan on the sensor device, no significant change occurs in the SPR angle ($\Delta\theta_{SPR} = 0.080°$) and frequency ($\Delta F_{SPR}$ =0.72 THz) due to no bonding reaction between the probe ligand and sensing target.

Based on chemical bonding between the probe ligand and sensing target, the chemical bonding configuration is changing, which leads to a change in the optical properties of the interface. If the concentration of formalin is increased, it forms more bonds with probe thus indicating greater interaction [55, 56]. Due to these greater interactions, more changes in the local refractive index near the composite layer interface are found. The amount of right shift of the SPR angle and F_{SPR} along rightwards with the increment of concentration of the detectable target ranging from 1000 nM to 1200 nM are illustrated in Fig. 3 and analytical data are listed in Table 2. The amount of changes would determine whether the formalin detection event would occur or not based on chemical bonding.

In the detection style, firstly, we found out the threshold values of $(\Delta R_{\min}^{p-t})$ & $(\Delta\theta_{SPR}^{p-t})$ and (ΔF_{SPR}^{p-t}) & $(\Delta T_{\max}^{p-t})$ from Table 2 by using the (5).

$$(\Delta R_{\min}^{p-t})_{Th} = \left| R_{\min}^{Probe} \sim R_{\min}^{Target} \right| = |0.0044\sim0.0062| = 0.0018 \quad (5a)$$

$$(\Delta\theta_{SPR}^{p-t})_{Th} = \left| \theta_{SPR}^{Probe} \sim \theta_{SPR}^{Target} \right| = |56.340\sim58.050| = 1.71 \quad (5b)$$

$$(\Delta T_{\max}^{p-t})_{Th} = \left| T_{\max}^{Probe} \sim T_{Max}^{Target} \right| = |0.3795\sim0.3981| = 0.0186 \quad (5c)$$

$$(\Delta F_{SPR}^{p-t})_{Th} = \left| F_{SPR}^{Probe} \sim F_{SPR}^{Target} \right| = |98.688\sim99.875| = 1.187 \quad (5d)$$

where $R_{\min}^{Probe}$ represents the minimum reflectance of probe ligand (chitosan), $R_{\min}^{Target}$ denotes the minimum reflectance of sampling target, θ_{SPR}^{Probe} depicts the SPR angle of probe ligand, and θ_{SPR}^{Target} is the SPR angle of sampling target. We reach the same conclusion by taking ΔF_{SPR}^{p-t} and $\Delta T_{\max}^{p-t}$ also as the detecting attributors.

Then we determine the change of the minimum reflectance, change of SPR angle, change of maximum transmittance, and change of F_{SPR} for different concentrated formalin molecules by using the data in Table 2 and tabulated them into Table 3.

Table 3 Change of $\Delta R_{\min}^{p-t}$, $\Delta T_{\max}^{p-t}$, ΔF_{SPR}^{p-t}, and $\Delta\theta_{SPR}^{p-t}$ values from (5) for different concentrations of dielectric formalin.

Concentration (C_a) (nM)	$\Delta R_{\min}^{p-t}(\%) = \lvert R_{\min}^{Probe} - R_{\min}^{Target} \rvert$	$\Delta\theta_{SPR}^{p-t}(\text{deg}) = \lvert \theta_{SPR}^{Probe} - \theta_{SPR}^{Target} \rvert$	$\Delta T_{\max}^{p-t}(dB) = \lvert T_{\max}^{Probe} - T_{\max}^{Target} \rvert$	$\Delta F_{SPR}^{p-t}(\text{THz}) = \lvert F_{SPR}^{Probe} - F_{SPR}^{Target} \rvert \rvert$
1000 (Target)	$(\Delta R_{\min}^{p-t})_{Th}$	$(\Delta\theta_{SPR}^{p-t})_{Th}$	$(\Delta T_{\max}^{p-t})_{Th}$	$(\Delta F_{SPR}^{p-t})_{Th}$
1001 (Target)	0.0022	2.04	0.0207	1.32
1010 (Target)	0.0026	2.33	0.0223	1.418
1100 (Target)	0.0038	3.15	0.0311	1.939
1110 (Target)	0.0041	3.34	0.0334	2.073
1200 (Target)	0.0056	4.28	0.0354	2.759

Table 4 Four probable conditions for making decision about successful interaction.

Conditions for using θ_{SPR} & $R_{\min}$ as detecting attributor	Conditions for using F_{SPR} & $T_{\max}$ as detecting attributor	Judgement
$\Delta R_{\min}^{p-t} \geqslant (\Delta R_{\min}^{p-t})_{Th}$ & $\Delta\theta_{SPR}^{p-t} \geqslant (\Delta\theta_{SPR}^{p-t})_{Th}$	$\Delta T_{\max}^{p-t} \geqslant (\Delta T_{\max}^{p-t})_{Th}$ & $\Delta F_{SPR}^{p-t} \geqslant (\Delta F_{SPR}^{p-t})_{Th}$	Formalin is detected
$\Delta R_{\min}^{p-t} \geqslant (\Delta R_{\min}^{p-t})_{Th}$ & $\Delta\theta_{SPR}^{p-t} \leqslant (\Delta\theta_{SPR}^{p-t})_{Th}$	$\Delta T_{\max}^{p-t} \geqslant (\Delta T_{\max}^{p-t})_{Th}$ & $\Delta F_{SPR}^{p-t} \leqslant (\Delta F_{SPR}^{p-t})_{Th}$	Reevaluate
$\Delta R_{\min}^{p-t} \leqslant (\Delta R_{\min}^{p-t})_{Th}$ & $\Delta\theta_{SPR}^{p-t} \geqslant (\Delta\theta_{SPR}^{p-t})_{Th}$	$\Delta T_{\max}^{p-t} \leqslant (\Delta T_{\max}^{p-t})_{Th}$ & $\Delta F_{SPR}^{p-t} \geqslant (\Delta F_{SPR}^{p-t})_{Th}$	Reevaluate
$\Delta R_{\min}^{p-t} \leqslant (\Delta R_{\min}^{p-t})_{Th}$ & $\Delta\theta_{SPR}^{p-t} \leqslant (\Delta\theta_{SPR}^{p-t})_{Th}$	$\Delta T_{\max}^{p-t} \leqslant (\Delta T_{\max}^{p-t})_{Th}$ & $\Delta F_{SPR}^{p-t} \leqslant (\Delta F_{SPR}^{p-t})_{Th}$	Free probe

If the measured values are greater than these threshold parameters, we observe the presence of formalin in that target sample. For clarifying detection conditions, we reach a conclusion according to Table 4. These values can really give an idea about successful interaction or the failed ones. The first condition in Table 4 expresses the desired condition, the second and third ones need careful recheck for attaining desired condition, and the fourth condition confirms that the probe is still free a target molecule.

3.2 Effect of different layers on sensor sensitivity

The sensor's performance is evaluated in terms of sensitivity (S) which is defined as [16, 18]:

$$S = \frac{\Delta\theta_{\mathrm{SPR}}}{\Delta n_{\mathrm{sens}}} = \frac{\Delta\theta_{\mathrm{SPR}}}{C_a}\frac{1}{\mathrm{d}n/\mathrm{d}c} \tag{6}$$

where $\Delta\theta_{\mathrm{SPR}}$ is the change of SPR angle due to the presence of formalin, and Δn_{sens} is the change of refractive index of the sensing dielectric after adsorption of formaldehyde molecules described in (2). The SPR angle shifts rightward in the SPR curve with the increment of refractive index followed by (1).

At the SPR point, the optical wave propagation constant which is represented by (3) must be equal to the surface wave propagation constant. It is known from (3) that the surface plasmon propagation constant changes according to the change of refractive index of sensing medium. Finally, it is observed that the SPR angle changing characteristics is responsible for the change of refractive index of sensing medium.

Firstly, in this section, we discuss the effect of inserting different layers on the detecting attributors such as the change of SPR angle and SPR frequency in the sensor configuration. Figs. 4(a) and 4(b) show the minimum reflectance (R_{min}) vs. SPR angle (θ_{SPR}) and the maximum transmittance (T_{max}) vs. F_{SPR} curves for different structures including the conventional structure and proposed structure at the refractive index n_{sens}=1.34 RIU (bare sensor). Figure 4 shows that the SPR angle and SPR frequency for the conventional layer biosensor are 54.36° and 94.1547 THz, respectively. Again, Fig. 4 shows that the SPR angle and SPR frequency with the graphene and gold metal layer based biosensor are 54.57° and 94.4015 THz, respectively. In this case, it can easily be observed that the change of SPR angle and SPR frequency for the conventional structure is very poor whereas the sensitivity with graphene but without TiO_2, SiO_2, and MoS_2 layers is consistently better than the conventional structure. This is due to the electron loss of graphene, which is accompanying with the imaginary dielectric constant. This increased SPR angle will lead to obtaining increased sensitivity of the sensor as sensitivity is directly proportional to the variation of the SPR angle discussed in [42–44] according to (6). Furthermore, Fig. 4 shows that the SPR angle and SPR frequency without TiO_2, SiO_2, and graphene but with MoS_2 layer are 55.60° and 95.5935 THz, respectively. This is because of MoS2's larger band gap [11, 18, 22, 42, 43], higher optical absorption efficiency [22–24], and larger work function (5.1 eV) as compared with graphene [11]. Further again, if both graphene and MoS_2 are used and TiO_2 and SiO_2 layers are not used, then Fig. 4 shows that the SPR angle and SPR frequency are 55.86° and 96.2495 THz, respectively. This is greater than the performance of using other materials due to the present of both characteristics of graphene and MoS_2. Furthermore, if the TiO_2-SiO_2 composite layer is used with the graphene and MoS_2, Fig. 4 shows that the SPR angle and SPR frequency are 55.90° and 96.9236 THz, respectively. Since TiO_2 and SiO_2 have a purely real refractive index, they can be used as an adherence layer above the prism base. As an adherence layer, the composite layer performs better than the individual TiO_2 and SiO_2 [16, 18] do because rich plasmon happens at the TiO_2-SiO_2 interface [18]. And this plasmon enhances light trapping effectively [32] which will generate more

surface plasmons (SPs). More surface plasmons (SPs) will enhance the SPR angle rightwards. An increase in the SPR angle will increase the SPR sensitivity. Lastly, the SPR angle and SPR frequency for the proposed structure are 56.26° and 97.968 THz, respectively, which reach the highest values among all the previous structures. Addition of probe molecules shifts the SPR angle rightwards due to the change of refractive index of the sensing dielectric. By adsorption of immobilized ions, an electron rich molecule would change in the sensing layer concentration which has led to a variation of the propagation constant.

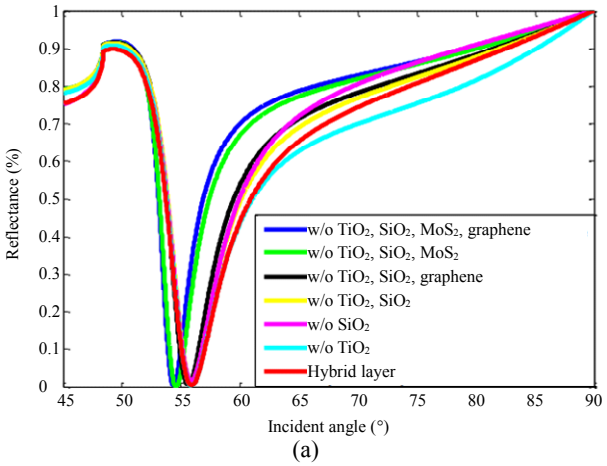

(a)

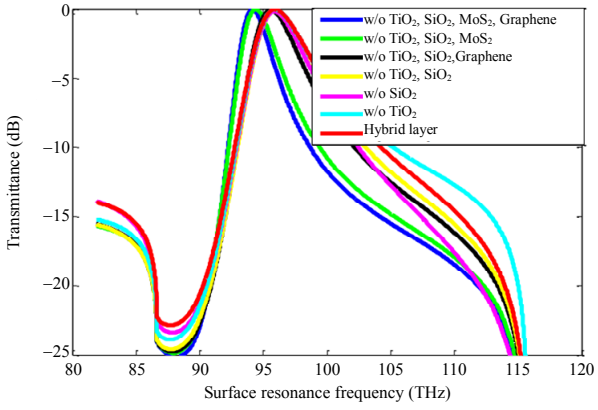

(b)

Fig. 4 SPR response curves of (a) reflectance (%) vs. incident angle (θ) curve and (b) transmittance (dB) vs. SPRF (THz) curve for different structures of biosensor.

Secondly, in this section, we represent the change of SPR angle with respect to the refractive index in Fig. 5. In Fig. 5, it is shown that the change of SPR angle with respect to RIU for the conventional structure and proposed different-layer structure. The change of SPR angle ($\Delta\theta_{SPR}$) for the conventional biosensor is very poor, which confirms a lower sensor sensitivity because the sensitivity is a proportionally dependent parameter of the change of SPR angle ($\Delta\theta_{SPR}$) as per the definition of sensitivity shown mathematically in (6). And for the proposed hybrid biosensor (Graphene & MoS_2 layer with TiO_2-SiO_2 porous nano particles), the change of SPR angle and SPR frequency are the maximum which confirm the highest sensitivity according to (6). Equation (2) shows how the SPR angle changes due to the change of molarity of the solution and refractive index. By this calibration, one can directly know the SPR angle of the system, just by measuring the refractive index (RI) of the sensing solution. The variation of the reflection intensity in accordance with the incident angle is plotted in Fig. 5. The reflectance curves at 1.34 RIU of sensing medium refractive index (bare sensor) and 1.41 RIU (present of formalin in sensor) are presented by solid and dashed lines of different colors, respectively. Here, the proposed structure (with all layers) is compared with some other structures including firstly the structure without TiO_2, SiO_2, MoS_2, and graphene layers (conventional structure), secondly the structure without TiO_2, SiO_2, and MoS_2 layers, thirdly the structure without TiO_2, SiO_2, and graphene layers, fourthly the structure without TiO_2 and SiO_2, fifthly the structure without TiO_2 layer, and finally the structure without SiO_2. The resonance angle (θ_{SPR}) at 1.34 RIU and 1.41 RIU of the sensing layer is calculated and then the sensitivity is measured. One can easily observe from Fig. 4 that the sensitivity increases gradually in accordance with the adding layers and it reaches the maximum with the hybrid structure of seven layers (proposed structure).

Thirdly, in this section, the shift of the SPR angle with the increment of refractive index having

a step size δC_n= 0.01 is measured and the corresponding increment of sensitivity of the proposed biosensor according to the (6) is also determined and graphically shown in Fig. 6.

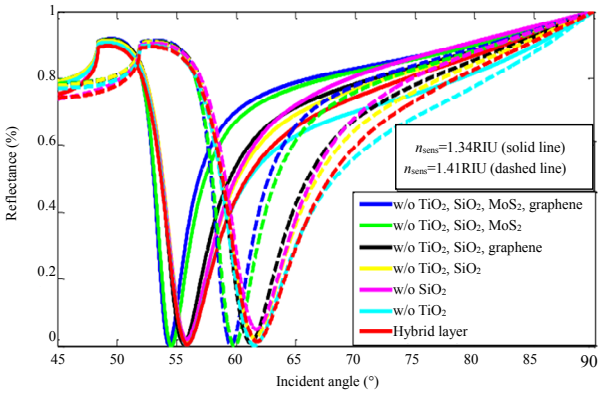

Fig. 5 Variation of the Reflection Intensity with respect to the incidence angle for different structures of SPR sensor.

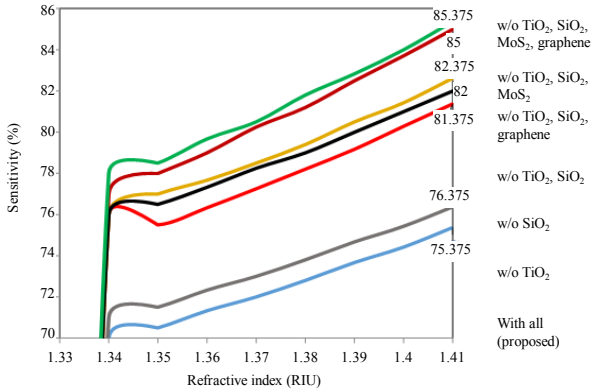

Fig. 6 Percentage of sensitivity vs. refractive index curve for different structures proposed.

From Fig. 6, firstly it is observed that the sensitivity for the conventional structure ranges from 70.44% to 75.375% with respect to the sensing medium refractive index ranging n_{sens}^{d} =1.34 RIU to n_{sens}^{d} =1.41 RIU, respectively. After then the sensitivity of the proposed structure with graphene but without TiO_2-SiO_2 and MoS_2 is investigated and it equals to a range from 71.62% to 76.375%, which is comparatively better than the conventional structure. Furthermore, the sensitivity of the structure with MoS_2 but without TiO_2-SiO_2 and graphene covers a range from 76.44% to 81.375%.

If both graphene and MoS_2 are used and TiO_2-SiO_2 are not used, the sensitivity is more improved than the previous structures whose sensitivity covers from 77% to 82.625%. Now, if the SiO_2 layer is used with grapheme and MoS_2 and TiO_2 is not used, the sensitivity enhances to a range from 78% to 85.00%.

If a TiO_2 layer is used instead of the SiO_2 layer in previous structures, just like before the sensitivity keeps almost constant. If we use all the layers at a time, which is a proposed structure in this work, the sensitivity is the highest among all the previous structures, which covers the range from 79% to 85.375%. Finally, in this section, the sensitivities for different structures are summarized in Table 5.

Table 5 Analysis of sensitivity corresponding to sensing layer refractive index at 1.41 RIU for seven different structures at the optimum thickness of TiO_2-SiO_2 and monolayer of MoS_2 and graphene.

Modeling structure	Sensitivity (%RIU^{-1})
Without TiO_2, SiO_2, MoS_2 and Graphene	75.26
Without TiO_2, SiO_2 and MoS_2 and with graphene	76.24
Without TiO_2, SiO_2 & graphene and with MoS_2	81.82
With graphene & MoS_2 and without TiO_2 & SiO_2	82.40
With graphene, SiO_2 & MoS_2 and without TiO_2	85.14
With graphene, TiO_2 & MoS_2 and without SiO_2	82.10
With graphene-MoS_2-TiO_2-SiO_2 (proposed)	85.375

3.5 References

In this paper, a numerical analysis is investigated to notice the consequence of adding of graphene, MoS_2, TiO_2, and SiO_2 layers step by step on sensitivity parameters for formalin detection. The first concern of this study is to detect the presence of the formalin based on the ATR method by noting the change of "SPR angle versus minimum reflectance" attributor and "F_{SPR} versus maximum transmittance" attributor. In this paper, chitosan is used as a probe legend to react with formalin (formaldehyde). The second concern is the sensitivity analysis by adding of graphene, MoS_2, TiO_2, and SiO_2 layers step by step. Graphene as well as MoS_2 thin films plays an important role in developing electro-optical sensor device due to their biocompatibility, high surface to volume ratio, low isoelectric point, and better chemical stability properties, which makes it very suitable for applications like formalin detection. For plasmonic effect near TiO_2-SiO_2 interface, the light

trapping is effectively enhanced because the enhanced light trapping more surface plasmons is generated which will eventually enhance the resonance angle, which can indeed satisfy the maximum sensitivity requirement. Numerically, the sensitivity of 85.375% with a refractive index of 1.41 RIU has been observed for the proposed sensor.

References

[1] M. B. Hossain, M. Hassan, L. F. Abdulrazak, M. M. Rana, M. M. Islam, and M. S. Rahman, "Graphene-MoS_2-Au-TiO_2-SiO_2 hybrid SPR biosensor for formalin detection: numerical analysis and development," *Advanced Materials Letters*, 2019, 10(9): 656–662.

[2] M. B. Hossain, M. M. Rana, L. F. Abdulrazak, S. Mitra, and M. Rahman, "Design and analysis of graphene-MoS_2 hybrid layer based SPR biosensor with TiO_2-SiO_2 nano film for formalin detection: numerical approach," *Optical and Quantum Electronics*, 2019, 51(6): 195–207.

[3] A. S. Sebaei, A. M. Gomaa, A. A. El-Zwahry, and E. A. Emara, "Graphene-MoS_2-Au-TiO_2-SiO_2 hybrid SPR biosensor: a new window for formalin detection," *International Journal of Analytical Chemistry*, vol. 2018, Article ID 2757941, 2018.

[4] N. Noordiana, A. B. Fatimah, and Y. C. Farhana, "Formaldehyde content and quality characteristics of selected fish and sea food from wet markets," *International Food Research Journal*, 2011, 18(1): 125–136.

[5] T. S. Yeh, T. C. Lin, C. C. Chen, and H. M. Wen, "Analysis of free and bound formaldehyde in squid and squid products by gas chromatography-mass spectrometry," *Journal of Food and Drug Analysis*, 2013, 21(2): 190–197.

[6] I. E. Bechmann, "Determination of formaldehyde in frozen fish with formaldehyde dehydrogenase using a flow injection system with an incorporated gel-filtration chromatography column," *Analytica Chimica Acta*, 1996, 320(2–3): 155–164.

[7] S. Ngamchana and W. Surareungchai, "Sub-millimolar determination of formalin by pulsed amperometric detection," *Analytica Chimica Acta*, 2004, 510(2): 195–201.

[8] M. B. Hossain, M. M. Rana, L. F. Abdulrazak, and S. Mitra, "Graphene-MoS_2 with TiO_2-SiO_2 layers based surface plasmon resonance biosensor: numerical development for formalin detection," *Biochemistry and Biophysics Reports*, 2019, 18: 100639.

[9] M. S. Rahman, M. S. Anower, M. K. Rahman, M. R. Hasan, M. B. Hossain, and M. I. Haque, "Modeling of a highly sensitive MoS_2-graphene hybrid based fiber optic SPR biosensor for sensing DNA hybridization," *Optik–International Journal for Light and Electron Optics,* 2017, 140: 989–997.

[10] M. B. Hossain and M. M Rana, "DNA hybridization detection based on resonance frequency readout in grapheme on Au SPR biosensor," *Journal of Sensors*, 2016, 16: 6070742–7.

[11] M. S. Rahmana, M. S. Anower, Md. R. Hasan, Md. B. Hossain, and M. I. Haque, "Design and numerical analysis of highly sensitive Au-MoS_2-graphene based hybrid surface plasmon resonance biosensor," *Optics Communications*, 2017, 396: 36–43.

[12] M. B. Hossain, T. B. A. Akib, L. F. Abdulrazak, and Md. M. Rana, "Numerical modeling of graphene-coated fiber optic surface plasmon resonance biosensor for BRCA1 and BRCA2 genetic breast cancer detection," *Optical Engineering*, 2019, 58(3): 037104.

[13] M. B. Hossain and M. M. Rana, "Graphene coated high sensitive surface plasmon resonance biosensor for sensing DNA hybridization," *Sensor Letters*, 2016, 14(2): 145–152.

[14] K. N. Shushama, M. M. Rana, R. Inum, and M. B. Hossain, "Graphene coated fiber optic surface plasmon resonance biosensor for the DNA hybridization detection: Simulation analysis," *Optics Communications,* 2017, 383: 186–190.

[15] M. M. Habib, R. Roy, M. M. Islam, M. Hassan, M. M. Islam, and Md. B. Hossain, "Study of graphene-MoS_2 based SPR biosensor with graphene based SPR biosensor: comparative approach," *International Journal of Natural Sciences Research*, 2019, 7(1): 1–9.

[16] M. B. Hossain, M. M. R. Khan, M. S. Rahman, S. S. B. Badrudduza, M. M. Sabiha, *et al*., "Graphene-MoS_2-Au-TiO_2-SiO_2 hybrid SPR biosensor: A new window for formalin detection," *Journal of Materials and Applications*, 2019, 8(2): 51–58.

[17] M. M. Islam, Md. M Islam, Y. C. Shimul, A. Rahman, A. A. Ruhe, M. Hassan, *et al*., "FDTD analysis fiber optic SPR biosensor for DNA hybridization: a numerical demonstration with graphene," *Journal of Materials and Applications,* 2019, 8(1): 13–19.

[18] M. B. Hossain, M. M. Islam, L. F. Abdulrazak, M. M. Rana, T. B. A. Akib, and M Hassan, "Graphene-

coated optical fiber SPR biosensor for BRCA1 and BRCA2 breast cancer biomarker detection: a numerical design-based analysis," *Photonic Sensors*, 2019, 9(4): 1–13.

[19] A. K. Mishra, S. K. Mishra, and B. D. Gupta, "SPR based fiber optic sensor for refractive index sensing with enhanced detection accuracy and figure of merit in visible region," *Optics Communications,* 2015, 344: 86–91.

[20] A. K. Mishra, S. K. Mishra, and B. D. Gupta, "Gas-clad two-way fiber optic SPR sensor: a novel approach for refractive index sensing," *Plasmonics*, 2015, 10(5): 1071–1076.

[21] A. K. Mishra, S. K. Mishra, and R. K. Verma, "Graphene and beyond graphene MoS_2: a New window in surface-plasmon-resonance-based fiber optic sensing," *The Journal of Physical Chemistry* C, 2016, 120(5): 2893–2900.

[22] A. K. Mishra and S. K. Mishra, "Infrared SPR sensitivity enhancement using ITO/TiO_2/silicon overlays," *Europhysics Letters*, 2015, 112(1): 10001.

[23] A. K. Mishra and S. K. Mishra, "MgF_2 prism/rhodium/graphene: efficient refractive index sensing structure in optical domain," *Journal of Physics*: *Condensed Matter*, 2017, 29: 145001.

[24] M. A. Habib, M. S. Anower, L. F. Abdulrazak, and M. S. Reza, "Hollow core photonic crystal fiber for chemical identification in terahertz regime," *Plasmonics*, 2019, 52: 101933.

[25] A. K. Mishra and S. K. Mishra, "Gas sensing in Kretschmann configuration utilizing bi-metallic layer of rhodium-silver in visible region," *Sensors and Actuators B: Chemical*, 2016, 237: 969–973.

[26] M. S. Rahman, M. S. Anower, and L. F. Abdulrazak, "Utilization of a phosphorene-graphene/TMDC heterostructure in a surface plasmon resonance-based fiber optic biosensor," *Photonics and Nanostructures-Fundamentals and Applications*, 2019, 35(3): 100711.

[27] W. Peng, Y. Liu, P. Fang, X. Liu, Z. Gong, H. Wang, *et al.*, "Compact surface plasmon resonance imaging sensing system based on general optoelectronic components," *Optics Express*, 2014, 22(5): 6174–6185.

[28] B. A. Prabowo, A. Purwidyantri, and K. C. Liu, "Surface plasmon resonance optical sensor: A review on light source technology," *Biosensors*, 2018, 8(3): 80.

[29] S. Unser, I. Bruzas, J. He, and L. Sagle, "Localized surface plasmon resonance biosensing: current challenges and approaches," *Sensors*, 2015, 15(7): 15684–15716.

[30] A. Ghamin, A. Rubaye, A. Nabok, and A. Tsargorodska, "LSPR biosensor based on nanostructured gold films: detection of mycotoxins," *Procedia Technology*, 2017, 27: 131–132.

[31] A. W. Wark, H. J. Lee, and R. M. Corn, "Long-range surface plasmon resonance imaging for bio affinity sensors," *Analytical Chemistry*, 2005, 77(13): 3904–3907.

[32] X. Zhao, X. Zhang, S. Z. Xiao, And W. S. Yi, "Long-range surface plasmon resonance sensor based on the GK570/Ag coated hollow fiber with an asymmetric layer structure," *Optics Express*, 2019, 27(7): 9550–9560.

[33] H. Fu, S. Zhang, H. Chen, and J. Weng, "Graphene enhances the sensitivity of fiber-optic surface plasmon resonance biosensor," *IEEE Sensors Journal*, 2015, 15(10): 5478–5482.

[34] K. F. Mak, C. Lee, J. Hone, J. Shan, and T. F. Heinz, "Atomically thin MoS_2: A new direct-Gap semiconductor," *Physical Review Letters*, 2010, 105(13): 136805.

[35] L. S. Oriol, D. Lembke, M. Kayci, A. Radenovic, and K. Andras, "Ultrasensitive photodetectors based on monolayer MoS_2," *Nature Nanotechnology*, 2013, 8(7): 497−501.

[36] M. Hernaez, "Nanostructured materials in optical fiber sensing," *The Open Optics Journal*, 2014, 7(1): 84−94.

[37] M. S. Rahman, M. S. Anower, L. F. Abdulrazak, and M. M. Rahman, "Modeling of a fiber-optic surface plasmon resonance biosensor employing phosphorene for sensing applications," *Optical Engineering*, 2019, 58 (3): 037103.

[38] A. Shalabney and I. Abdulhalim, "Electromagnetic fields distribution in multilayer thin film structures and the origin of sensitivity enhancement in surface plasmon resonance sensors," *Sensor Actuators A: Physal*, 2010, 159(1): 24–32.

[39] J. B. Maurya, Y. K. Prajapati, V. Singh, and J. P. Saini, "Sensitivity enhancement of surface plasmon resonance sensor based on grapheme-MoS_2 hybrid structure with TiO_2-SiO_2 composite layer," *Applied Physics A*, 2013, 121(2): 525–533.

[40] J. Homola and M. Piliarik, "Surface plasmon resonance based sensors," *Springer*, 2006, 4(2), 46–47.

[41] K. N. Shushama, M. M. Rana, R. Inum, and M. B. Hossain, "Sensitivity enhancement of graphene coated surface plasmon resonance biosensor," *Optical and Quantum Electronics*, 2017, 49(11): 381.

[42] L. M. Wu, J. Guo, X. Y. Dai, Y. J. Xiang, and D. Y. Fan, "Sensitivity enhanced by MoS_2-graphene hybrid structure in guided-wave surface plasmon resonance biosensor," *Plasmonics*, 2018, 13(1): 281–285.

[43] L. Wu, Y. Jia, L. Y. Jiang, J. Guo, X. Y. Dai, Y. J. Xiang, *et al.*, "Sensitivity improved SPR biosensor based on the MoS_2/graphene-aluminum hybrid structure," *Journal of Lightwave Technology*, 2017, 35(1): 82–87.

[44] L. M. Wu, J. Guo, Q. K. Wang, S. B. Lu, X. Y. Dai,

Y. J. Xiang, *et al.*, "Sensitivity enhancement by using few-layer black phosphorus-graphene/TMDCs hetero structure in surface plasmon resonance biochemical sensor," *Sensors and Actuators B: Chemical*, 2017, 249: 542–548.

[45] V. Ball and J. J. Ramsden, "Buffer dependence of refractive index increments of protein solutions," *Biopolymers*, 1998, 46(7): 489–492.

[46] L. Diéguez, N. Darwish, M. Mir, E. Martínez, M. Moreno, and J. Samitier, "Effect of the refractive index of buffer solutions in evanescent optical biosensors," *Sensor Letters*, 2009, 7(5): 851–855.

[47] M. B. Hossain and S. Muktadhir, "Multi-structural optical devices modeling using graphene tri-layer sheets," *Optik*, 2016, 127(15): 5841–5851.

[48] M. B. Hossain, M. S. Muktadhir, and M. M. Rana, "Modeling graphene macroscopic and microscopic conductivity in the sub-cell FDTD method," in *International Conference on Electrical & Electronic Engineering (ICEEE)*, Rajshahi, Bangladesh, 2015.

[49] M. M. Rana, M. B. Hossain, M. R. Islam, and Y. G. Guo, "Surface plasmon polariton propagation modeling for graphene parallel pair sheets using FDTD," in *2015 IEEE International Conference on Applied Superconductivity and Electromagnetic Devices (ASEMD)*, Shanghai, China, 2015.

[50] M. B. Hossain and M. M. Rana, "An effective compact-FDTD wideband modeling of graphene conductivity," in *2015 International Conference on Electrical Engineering and Information Communication Technology (ICEEICT)*, Dhaka, Bangladesh, 2015.

[51] M.A. Habib, M.S. Reza, L.F. Abdulrazak and M.S. Anower, "Extremely high birefringent and low loss microstructure optical waveguide: Design and analysis," *Optics Communications*, 2019, 446: 93–99.

[52] C. Nylander, B. Liedberg, and T. Lind, "Gas detection by means of surface plasmons resonance," *Sensors and Actuators*, 1982, 3: 79–88.

[53] A. J. C. Tubb, F. P. Payne, R. B. Millington, and C. R. Lowe, "Single mode optical fiber surface plasma wave chemical sensor," *Sensors and Actuators B,* 1997, 41(1–3): 71–79.

[54] U. Fano, "The theory of anomalous diffraction gratings and of quasi-stationary waves on metallic surfaces (Sommerfeld's waves)" *Journal of the Optical Society of America*, 1941, 31(3): 213–222.

[55] R. L. Earp and R. E. Dessy, "Surface plasmon resonance", in *Commercial Biosensors: Applications to Clinical, Bioprocess, and Environmental Samples*. New York: John Wiley and Sons, 1998.

[56] M. S. Rahman, S. S. Noor, M. S. Anower, L. F. Abdulrazak, M. M. Rahman, and K. A. Rikta, "Design and numerical analysis of a graphene-coated fiber-optic SPR biosensor using tungsten disulfide," *Photonics and Nanostructures-Fundamentals and Applications*. 2019, 33: 29–35.